Analytical and Bioanalytical Chemistry
https://doi.org/10.1007/s00216-018-1336-8

RESEARCH PAPER

Minimally invasive technique for measuring transdermal glucose with a fluorescent biosensor

Sheniqua Brown[1] · Paige N. Zambrana[2] · Xudong Ge[1] · Dayanand Bagdure[3] · Audra L. Stinchcomb[2] · Govind Rao[1] · Leah Tolosa[1]

Received: 15 June 2018 / Revised: 15 August 2018 / Accepted: 17 August 2018

Abstract

There is a need for blood glucose monitoring techniques that eliminate the painful and invasive nature of current methods, while maintaining the reliability and accuracy of established medical technology. This research aims to ultimately address these shortcomings in critically ill pediatric patients. Presented in this work is an alternative, minimally invasive technique that uses microneedles (MN) for the collection of transdermal glucose (TG). Due to their comparable skin properties, diffusion studies were performed on full thickness Yucatan miniature pig skin mounted to an in-line diffusion flow cell and on different skin sites of human subjects. Collected TG samples were measured with a L255C mutant of the *E. coli* glucose-binding protein (GBP) with an attached fluorescent probe. The binding constant ($K_d = 0.67$ μM) revealed the micromolar sensitivity and high selectivity of the his-tagged GBP biosensor for glucose, making it suitable for TG measurements. In both the animal and human models, skin permeability and TG diffusion across the skin increased with MN application. For intact and MN-treated human skin, a significant positive linear correlation ($r > 0.95$, $p < 0.01$) existed between TG and BG. The micromolar sensitivity of GBP minimized the volume required for interstitial fluid glucose analysis allowing MN application time (30 s) to be shortened compared to other studies. This time reduction can help in eliminating skin irritation issues and improving practical use of the technique by caregivers in the hospital. In addition, the his-tagged optical biosensor used in this work can be immobilized and used with a portable sensing fluorometer device at the point of care (POC) making this minimally invasive technology more ideal for use in the pediatric intensive care unit.

Keywords Optical biosensor · In-line flow through diffusion cell · Transdermal glucose monitoring · Microneedles

Introduction

Blood glucose monitoring is a critical component in the management of critically ill children in the pediatric intensive care unit (PICU) [1]. Current FDA-approved practices for glucose monitoring require painful and invasive blood draws that are analyzed either in the laboratory or by handheld bedside meters. Continuous glucose monitoring (CGM) devices are being studied as an alternative in the management of critically ill children [2–5]; however, CGM devices involve inserting a probe into the subcutaneous layer, beneath the skin, and can be painful, uncomfortable, and traumatizing for young children [6–9]. Thus, there is interest in devices which are more effective and less invasive to monitor blood glucose levels. Eliminating the pain and discomfort associated with the aforementioned practices can be advantageous to young patients, their parents, and their caregivers. In a typical example, management of a 3-year-old PICU patient with diabetic ketoacidosis (DKA), having an initial blood glucose of 1317 mg/dL, required blood glucose monitoring 55 times over a 48-h period. A painless alternative will allow the bedside nurse to collect glucose data with minimal disturbance to such a patient, especially in the middle of the night. In addition, glucose levels ranging from as low as 13 mg/dL to as high as

✉ Leah Tolosa
leah@umbc.edu

[1] Center for Advanced Sensor Technology Research (CAST), Department of Chemical, Biochemical and Environmental Engineering, University of Maryland Baltimore County (UMBC), 1000 Hilltop Circle, Baltimore, MD 21250, USA

[2] Department of Pharmaceutical Sciences, University of Maryland, 20 North Pine Street, Baltimore, MD 21201, USA

[3] Department of Pediatrics, University of Maryland Medical Center, 110 S Paca Street, Baltimore, MD 21201, USA

Published online: 31 August 2018

1800 mg/dL have been observed in the PICU [10, 11]. This demonstrates the need for a minimally invasive glucose sensing device that is painless, bloodless, safe, and has a wide range of detection.

The development of ligand-specific periplasmic binding proteins as optical biosensors for measuring glucose has been explored for noninvasive sensing, as well as sensing in clinically relevant ranges [12–18]. The sensor preparation involves using the *E. coli* glucose-binding protein (GBP) that undergoes a large conformational change from an open ligand-free structure to a closed glucose-bound structure [19]. This structural change allows GBP to be used as an optical biosensor when a polarity sensitive fluorescent probe, acrylodan (Acr), is attached to a cysteine mutation site responsive to glucose binding [20, 21]. In the presence of micromolar glucose concentrations, the emission of the bound Acr (510 nm) is quenched and a spectrophotometer is used to observe the glucose-associated fluorescence changes. Previous work reveals GBP having significantly less sensitivity to other sugars (< 10% response) in comparison with glucose (~ 35%); however, it responds to galactose (25%). With the exception of galactosemia patients and some newborns having elevated galactose, blood and interstitial fluids have negligible amounts of these sugars in comparison with glucose and are not expected to interfere [12]. Due to its high selectivity and specificity for glucose, the GBP biosensor was used in a noninvasive sensing technology that exploits the thin, immature neonatal skin [14, 22, 23]. It has also been used to successfully monitor blood glucose in adults through noninvasive transdermal glucose (TG) measurements [22].

In this work, we introduce microneedles (MNs) as a minimally invasive tool to increase skin permeability and improve diffusion of glucose across skin. MNs are microscopic needles capable of creating micrometer-sized channels in the skin [24]. They penetrate the stratum corneum, the outermost dead skin layer, and have been used to enhance transdermal drug delivery (TDD) by eliminating permeability limitations associated with the presence of the stratum corneum [25, 26]. Using MNs have proven to increase human skin permeability up to four orders of magnitude [27]. Studies have shown the success of using MNs as a tool to collect and measure glucose from interstitial fluids (ISF); however, some strategies rely on ISF extraction via vacuum suction [28] or swelling of hydrogel MNs [29–33] to collect millimolar concentrations detectable by current electrochemical-based sensors. MN techniques that use off-device analysis have challenges with prolonged extraction times, required ISF transfer for analysis, and low ISF volume collection or evaporation causing measurement variability and error [34]. Hollow silicon microneedles integrated with enzymatic glucose sensors were designed for on-device analysis eliminating need to transfer ISF [35–38]; however, they still require long collection times for microliter volumes and detectable concentrations, as well as the need to transfer fluid to the backside of MNs for analysis. For CGM, hollow MNs with a buffer filled sensing chamber were designed to allow passive diffusion of glucose from ISF to sensor eliminating ISF extraction step and allowing real-time bioanalysis [39–41]. Although most promising, many of these devices require millimolar glucose concentrations for analysis.

In this work, we present a minimally invasive technique that uses MNs to collect TG samples that are measured with our micromolar sensitive glucose biosensor. The effects of MN implementation on TG detection are determined in an in vitro pig skin model that is representative of blood flow beneath the human skin, as well as preliminary studies on healthy adult human subjects. Both pig and human skin used have comparable properties to the fully developed skin of children.

Materials and methods

D-Glucose (99.5 + %), guanidine hydrochloride (GuHCl), and sodium phosphate monobasic monohydrate ($NaH_2PO_4 \cdot H_2O$) were obtained from Sigma-Aldrich (St. Louis, MO). Isopropyl β-D-1-thiogalactopyranoside (IPTG), urea, TrisHCl, potassium phosphate monobasic, and potassium phosphate dibasic (99.0 + %) were obtained from Fisher Scientific (Fair Lawn, NJ). Nanopure water from an in-house Milli-Q system (EMD Millipore; Billerica, MA) was used.

GBP preparation and fluorophore labeling

The polyhistidine-tagged GBP biosensor was prepared similarly to H152C GBP biosensor described by Tiangco et al. [23]. In this work, the L255C GBP mutant was overexpressed in BL21 competent *Escherichia coli* cells through induction with 1 M IPTG in 1 L of LB medium. The resulting cell pellet was lysed with sonication (Fisher Scientific Sonic Dismembrator Model 500) in lysis buffer at pH 8 containing 6 M GuHCl, 10 mM TrisHCl, and 100 mM $NaH_2PO_4 \cdot H_2O$. Centrifugation was then used to separate the soluble protein. For purification, the supernatant went through immobilized metal affinity chromatography (IMAC) with 5 mL of nickel nitrilotriacetic acid (Ni-NTA) agarose resin. The protein was washed and eluted with buffers containing 8 M urea, 10 mM TrisHCl, and 100 mM $NaH_2PO_4 \cdot H_2O$. Upon elution from the IMAC column, GBP concentration was estimated using the Bradford protein assay and presence was confirmed with SDS-PAGE. The highly pure fractions were pooled and dialyzed in 20 mM phosphate buffer at pH 7.4. Protein labeling with Acr fluorescence probe involved a 10-fold dropwise addition of tris(2-carboxyethyl)phosphine (TCEP) stock solution mixed for an hour, followed by the addition of 10-fold

of Acr stock solution mixed for 2 h at room temperature. For removal of excess dye, the labeled protein was passed through a G-25 Sephadex size exclusion chromatography column. Fractions containing fluorescently labeled GBP were pooled, sterilized with 0.22 μm filters, and stored at 4 °C.

Biosensor calibration, sensitivity determination, and glucose assay

Fluorescence measurements of GBP were taken in a 96-well plate using the SpectraMax M5 spectrophotometer (Molecular Devices, San Jose, CA). Five microliters of D-glucose standards, ranging from 4 to 200 μM, was added to the GBP biosensor. After each addition, the fluorescence intensity was measured and the normalized change in fluorescence intensity with respect to glucose concentration was determined. The normalized change in fluorescence (ΔF) was defined as:

$$\Delta F = \frac{F_0 - F}{F_0} \tag{1}$$

where F is the fluorescence intensity of ligand bound protein and F_0 is the fluorescence intensity of ligand-free protein. This information was used to create a standard saturation curve relating substrate concentration to the normalized fluorescence response of the GBP biosensor. The highly sensitive linear range of the saturation curve was used for quantification of μM levels of glucose in transdermal skin samples. In addition, as described in previous work, nonlinear regression of the saturation curve is used to calculate the apparent binding constant (K_d) of GBP to determine the biosensor's sensitivity and capability to detect and measure trace amounts of glucose present in transdermal samples [13, 22, 42].

For sample analysis, collected transdermal samples were added in 5 μL increments to 200 μL of the GBP biosensor in a 96-well plate. After each addition, the fluorescence intensity was measured, and normalized fluorescence change determined. Sample addition continued until readings were well above the biosensor's limit of quantification (LOQ). The measured fluorescence changes along with the sensitive range of the standard curve were used for quantification of glucose concentration in transdermal samples.

Transdermal glucose diffusion studies

Pig skin preparation and flow cell setup

Full thickness Yucatan miniature pig skin was purchased from Sinclair BioResources (Auxvasse, MO). Upon arrival on ice, the skin was dermatomed to a thickness of 1.4 ± 0.25 mm using a Padgett dermatome to remove fat, leaving viable epidermis and dermis. The skin was then wrapped in aluminum foil, sealed in a plastic bag, and stored at − 20 °C until ready to use. Before each experiment, the skin was thawed to room temperature, cut into 4.84 cm^2 pieces, and placed onto membrane supports in in-line diffusion cells (PermeGear, Inc., Hellertown, PA) with epidermis side facing the donor chamber. Setup contained a diffusion area of 0.95 cm^2. The skin was maintained at a temperature of 33 ± 1 °C with a circulating jacketed water bath. Flow cell setup described by Tiangco et al. was used (Fig. 1) [23] with the application of a MN array insert on a vibrating pen to the stratum corneum of the skin in the donor chamber.

Theoretical model development for TG diffusion through pig skin

Simulation analysis of the unsteady-state diffusion of glucose across pig skin described in the flow cell setup was performed. The unsteady one-dimensional glucose diffusion across pig skin can be expressed by

$$\frac{\partial C(x,t)}{\partial t} = D\frac{\partial^2 C(x,t)}{\partial x^2} \tag{2}$$

Where $C(x, t)$ is the glucose concentration in the pig skin, D is the diffusion coefficient of glucose, t is the time, and x is the distance from the surface of the pig skin contacting the standard glucose solution. The initial condition inside the pig skin before the measurement is:

$$C(x,0) = 0 \tag{3}$$

During the measurement, one side contacts a solution with a glucose concentration of C_0, and the other side is kept at zero concentration (strictly speaking, C (L,0) is not zero, but extremely low so negligible compared to C_0). This gives the boundary conditions

$$C(0,t) = C_0 \;\; and \;\; C(L,0) = 0 \tag{4}$$

The solution of Eq. (2) with initial condition of Eq. (3) and boundary condition of Eq. (4) is as follows

$$C(x,t) = C_0\left[1 - \frac{x}{L} - \sum_{i=1}^{\infty}\frac{2}{\pi i} sin\left(\frac{i\pi x}{L}\right) exp\left(-\frac{i^2 D\pi^2 t}{L^2}\right)\right] \tag{5}$$

The first derivative of C (x, t) with respect to x equals to

$$\frac{\partial C(x,t)}{\partial x} = -\frac{C_0}{L}\left[1 + 2\sum_{i=1}^{\infty} cos\left(\frac{i\pi x}{L}\right) exp\left(-\frac{i^2 D\pi^2 t}{L^2}\right)\right] \tag{6}$$

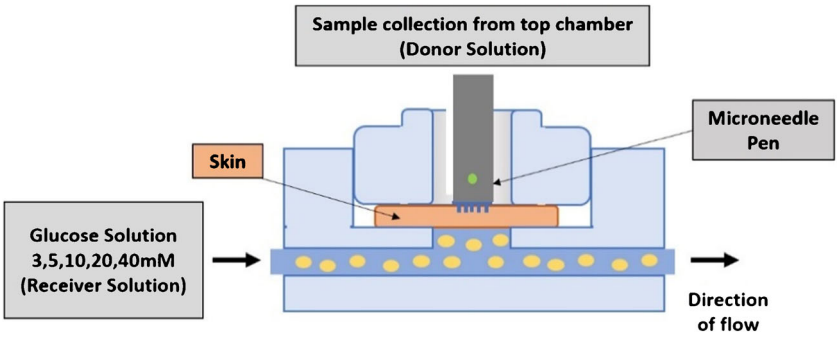

Fig. 1 Flow cell setup for transdermal glucose diffusion studies on pig skin using MN array

The glucose mass flux from the pig skin to the collection buffer, F, can be calculated by,

$$F = -DA\frac{\partial C(x,t)}{\partial x}\bigg|_{x=L} = V_L\frac{dC_L}{dt} \tag{7}$$

Where A is the sampling area, V_L is the volume of the sampling buffer, and C_L is the glucose concentration in the sampling buffer. Integrating Eq. (7) from t_1 to t_2, we get

$$\frac{C_L}{C_0} = \frac{DA}{LV_L}(t_2 - t_1) - \frac{2AL}{\pi^2 V_L}\sum_{i=1}^{\infty}\frac{cos(i\pi)}{i^2} \left[exp\left(-\frac{i^2 D\pi^2 t_2}{L^2}\right) - exp\left(-\frac{i^2 D\pi^2 t_1}{L^2}\right)\right] \tag{8}$$

From the above equation, we can see that the ratio of C_L to C_0 is independent of C_0. Therefore, the ratio of C_L to C_0 will follow the same trend no matter what glucose concentration is used. Using set parameter values based on experimental protocol ($A = 0.95$ cm^2, $D = 1.5 \times 10^{-7}$ cm^2/s, $L = 0.14$ cm, $V_L = 0.25$ cm^3, washing time = 5 min, drying time = 10 min, sampling time = 15 min), the glucose concentrations in the samples were compared between intact pig skin and after MN application.

TG diffusion studies using MNs on pig skin model

For all the in vitro permeation tests (IVPT), diffusion cells were filled with a receiver[1] solution of filtered phosphate-buffered saline pH 7.4 (PBS). The skin was allowed to equilibrate for 30–45 min, after which trans-epidermal water loss (TEWL) values were obtained using a cyberDerm RG-1 open chamber evaporimeter (cyberDERM, Inc.; Broomall, PA) in order to confirm skin integrity. Any skin with TEWL values higher than 15.0 g/m^2 h was deemed unfit and replaced. Initial TEWL studies investigated the effects of MN number (9 or 36-count), length (250 or 500 μm), and application time on skin permeability to determine ideal MN parameters for IVPT experiments on pig skin. A motorized vibrating MN pen (Dr. Pen Ultima A6) was used on pig skin. The device consisted of an array of medical grade stainless steel MNs having a base diameter of 0.2 mm and an application area of approximately 90 mm^2. After MN parameters were selected, a minimally invasive sampling protocol was used to collect TG through the pig skin.

For the minimally invasive sampling protocol, 250 μL of PBS was pipetted onto the epidermal side of the skin into the donor[1] chamber to wash the skin removing any excess glucose on the surface. After 5 min, the PBS on top of the skin was removed, discarded and the skin was allowed to dry with a fan for 10 min. After drying, the vibrating MN pen with a disposable tip of 36-count MN array insert was held on top of the epidermal side of the skin for 30 s with a penetrating depth of 250 μm to allow the formation of diffusion channels. TEWL values were recorded again with the expectation of a doubling effect from the original TEWL values taken prior to MN puncture. After a successful doubling in TEWL value was seen, 250 μL of PBS was placed on the epidermal side of the skin for 15 min before being removed and collected as a baseline glucose reading.

After baseline was taken for each cell, receiver solution was changed in order to contain either 3, 5, 10, 20, or 40 mM glucose in PBS, corresponding to 54, 90, 180, 360, and 720 mg/dL, respectively. The skin was wiped with an alcohol swab and washing procedure was performed again. After drying 250 μL of PBS without glucose was added to the donor chamber and allowed to sit for 15 min before collection. The washing, drying, and sample collection process was performed six times allowing for collection of glucose diffusion samples every 30 min for 3 h. System was run at a flow rate of approximately 1 mL/h to maintain constant glucose concentrations under the skin as glucose diffusion to the donor chamber occurred. Upon collection, all samples were immediately stored at −20 °C until analysis with GBP biosensor to prevent degradation of glucose.

[1] Receiver and donor solutions are conventional designations for in vitro topical drug delivery experiments where the drug (donor) diffuses from the epidermal side of the skin to the flow solution (receiver). In our experiments, glucose diffuses from the flow solution to the epidermal side.

TG diffusion studies using MNs on healthy adults

All subjects gave their informed oral consent for inclusion before they participated in the study. The study was conducted in accordance with the Declaration of Helsinki, and the protocol was approved by the Office of Research Protections and Compliance of UMBC (Protocol Y17LT05060) on November 9, 2016. Initial diffusion studies on healthy adult subjects focused on determining ideal site for MN application. The TEWL was measured at two different skin sites (fingertip or forearm), while varying number (9 or 36-count), length (250 or 500 μm), and application time of MNs. The permeability results were used to determine application site and MN parameters to be used in further studies. TG samples on adults were additionally collected using a modified version of the protocol described in the pig skin studies. TG samples and TEWL measurements for intact and MN-treated skin were collected from the forearm of healthy adult subjects during two scenarios. The first study was conducted during a fasting phase in which transdermal samples were collected for uncompromised skin, as well as skin treated with an array of 9 and 36-count MNs.

The second study looked at collecting TG samples during an oral glucose tolerance test (OGTT) in which subjects were asked to fast 12 h prior to the start of the study. For the OGTT, transdermal samples were collected during the fasting phase separated by a 30-min interval. The subject then consumed 75 g of food grade glucose purchased from The Science Company (Lakewood, CO). After ingestion of glucose, another four to five transdermal samples were collected over a 3-h period. At the start of the study, the skin was equilibrated in the testing area for 30 min, and then the TEWL of the sampling area was measured with a VapoMeter (Delfin Technology, Finland). The transdermal sampling protocol for intact skin (no MN application) involved first cleaning the skin area with an alcohol swab and then washing the skin with PBS pH 7.4 at 37 °C for 5 min. The skin was then dried with air for 2 min. Two hundred fifty microliters of PBS in an Eppendorf tube was inverted and placed on the skin surface for 5 min to allow for the passive diffusion of glucose into sample solution. After each TG sample collection, the blood glucose was measured using a ReliOn Confirm™ Blood Glucose Meter. For MN-treated skin, the same protocol was followed with the addition of MN treatment for 30 s using the vibrating MN pen prior to transdermal sample collection with an Eppendorf tube containing PBS. To ensure MN penetration, the TEWL values were measured prior to and after MN application. The collected transdermal samples were immediately stored at − 20 °C until testing with the GBP biosensor.

Results and discussion

Biosensor

The his-tagged L255C GBP biosensor was prepared and the apparent dissociation constant, K_d, was calculated by nonlinear regression on the saturation curve for one binding site. K_d was found to be 0.67 ± 0.05 μM (average ± standard deviation). The submicromolar K_d confirms sufficient biosensor sensitivity at the low concentrations associated with TG. Figure 2 shows that the most sensitive and linear range of the GBP biosensor can be found at concentrations < 1 μM, following the trend $[y = (0.102 \pm 0.006)x + (0.007 \pm 0.003)]$. There is a significant positive correlation between the micromolar glucose concentrations and normalized fluorescence response (correlation coefficient, $r = 0.992$; probability, $p < 1 \times 10^{-4}$; confidence interval, CI = 99.99%). Interpolation within the highly sensitive region of the calibration curve is used to calculate the glucose concentrations found in the collected transdermal samples for pig and human skin. It is important to note that although fluorescence response of labeled protein was consistent for an individual protein batch, variation from batch to batch can occur as a result of variances in, e.g., the degree of labeling, the efficiency of removing unreacted dye, etc. For this reason, the protein was calibrated, and a response curve was generated each time samples were analyzed.

TG diffusion studies

In vitro pig skin theoretical model

The glucose diffusion through the pig skin was simulated using a model for unsteady-state diffusion (Eq. (8)) and the

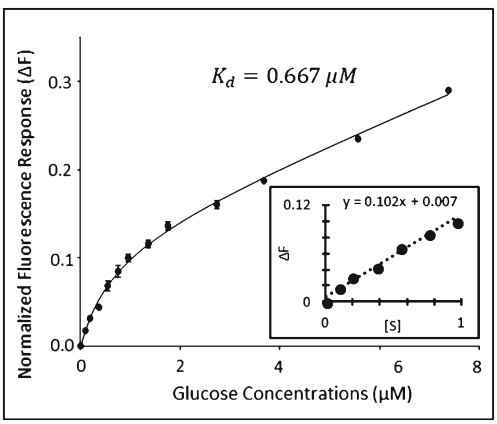

Fig. 2 Saturation curve for GBP biosensor used to determine K_d with nonlinear fit model; Inset: Highly sensitive range at lower concentrations revealing micromolar sensitivity and positive linear correlation following the trend $y = (0.102 \pm 0.006) + (0.007 \pm 0.003)$ with a correlation coefficient of 0.992

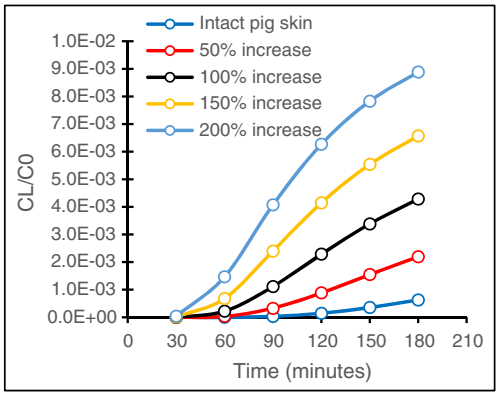

Fig. 3 Effect of diffusion coefficient on the calculated glucose concentrations in the samples for intact pig skin and after MN application

results are shown in Fig. 3. In the simulation results, the ratio of C_L to C_0 is independent of C_0 and there is almost no glucose in the first sample. Compared to the actual experimental data given in Fig. 5b, which show a base glucose concentration at about 4 μM, these simulation results do not closely match. This disagreement may be due to the oversimplification of the model as initial zero glucose concentration was assumed and no glucose production or consumption during the measurement was considered in simulation. In reality, there may be some residual glucose in the pig skin. Glucose is known to be a product of skin maturation.

Despite the discrepancy, the overall trend is the same. The calculated glucose concentrations in the samples are significantly higher after MN application. Overall, the glucose concentration in the samples increases with time following an S-shaped curve, but closer to linear for the first few samples. When steady-state diffusion is reached, the glucose concentration in the samples remains constant. As MN application can increase the glucose diffusion coefficient, these simulated results confirm the effects of MN application on the glucose concentration in the samples. This model can be used to guide the experiments by simulating the effects of factors such as the glucose diffusion coefficient, skin thickness, and sample volume.

Diffusion studies on pig skin model

The first set of diffusion studies using the MN pen was conducted on an in vitro model consisting of pig skin mounted in an in-line diffusion flow cell. Pig skin is commonly used for estimation of in vitro human skin permeation behavior because they have similar surface lipids, barrier thickness, and morphological aspects [43]. Before initiation of the IVPT pig skin experiments, the cyberDerm evaporimeter was used to measure the TEWL of pig skin, while varying the MN number and length, to determine MN effects on skin permeability. In addition, skin permeability changes were used to select optimum MN parameters for TG pig skin studies (Table 1). As the number and length of MNs increased so did the TEWL, or skin permeability. The skin permeability data revealed that a 36 MN array insert having a length of 250 μm and being applied for 30 s produced the most stable TEWL measurements while keeping MN length at a minimum, making these parameters most ideal for IVPT studies on pig skin.

After the optimum MN parameters were determined, TG was collected on the pig skin. For this study, it is important to note that a constant pump rate of 1 mL/h and constant tubing size were used; therefore, variations in pressure between the cells used for sample collection should not exist. Previous work looked at the effects of osmotic pressure on flux within the IVPT system [44]. When the viscosity of the donor solutions was kept constant and osmotic pressure varied, the resulting flux values showed no trend corresponding to varying osmotic pressure within the system; therefore, if slight variances in pressure occurred, they would have no effect on sample collection.

The pig skin used for the IVPT had an average thickness of 1.34 ± 0.11 mm. In addition, TEWL values were measured with the cyberDerm evaporimeter to confirm MN penetration through the full thickness pig skin. During the in vitro TG diffusion studies, the permeability of the skin was seen to increase with the use of MNs on the skin surface. TEWL of uncompromised intact skin was measured to be on average 5.1 ± 1.1 g m^{-2} h^{-2} while the skin treated with an array of 36 MNs for 30 s was measured at 23.14 ± 6.48 g m^{-2} h^{-2}. The more than four times increase in TEWL with MN application confirmed the successful penetration of the pig skin and increased permeability with this minimally invasive technique.

The GBP biosensor was then used to measure TG samples collected every 30 min through full thickness pig skin over a 3-h testing period. Glucose solutions corresponding to 3, 5, 10, 20, and 40 mM concentrations flowed under the dermal side of the skin in the receiver chamber of the cell, all of which are clinically significant blood glucose concentrations in the pediatric age group. Transdermal samples were collected from intact and MN-treated skin. Figure 4 compares the TG concentrations of intact skin to MN-treated skin for each millimolar glucose concentration tested. For all millimolar glucose concentrations, there is a statistically significant difference observed between the measured TG of intact and MN-treated skin ($p \leq 0.02$, CI = 98%). The biosensor can differentiate between the intact and MN skin when looking at individual mM concentrations, even at very low concentrations. This distinction becomes more evident as the glucose concentration of the receiver solution increases moving from approximately a unit increase at lower concentrations (3 mM: 4.3 ± 0.15 to 5.6 ± 0.59 μM) to an almost seven times increase at higher concentrations (40 mM: 3.6 ± 0.08 to 25.9 ± 9.46 μM).

When keeping the skin treatment constant (intact or MN) and varying the receiver glucose concentrations, we see the benefit of the MN implementation. Figure 5a shows that when looking at the TG of intact uncompromised skin samples, no significant distinction can be made between the wide range of

Table 1 Effects on TEWL, or permeability of pig skin while varying MN length, number, and time of application

		TEWL (g/m^2*h)	Standard deviation
9 MN array, 500 μm			
Trial 1 (30 s)	Baseline (no MN)	3.13	0.03
Skin thickness 1.50 mm	MN	7.74	0.15
Trial 2 (30 s)	Baseline	3.22	0.07
Skin thickness 1.19 mm	MN	6.45	0.12
36 MN array, 250 μm			
Trial 1 (30 s)	Baseline	3.13	0.15
Skin thickness 1.29 mm	MN	26.00	0.10
Trial 2 (30 s)	Baseline	3.00	0.11
Skin thickness 1.53 mm	MN	24.78	0.19
36 MN array, 500 μm			
Trial 1 (30 s)	Baseline	2.26	0.11
Skin thickness 1.33 mm	MN	29.74	0.13
Trial 2 (30 s)	Baseline	2.81	0.13
Skin thickness 1.56 mm	MN	44.00	0.40

glucose concentrations ($p > 0.05$). Since full thickness skin is being used and the stratum corneum is still present to act as a permeability limitation, a longer sampling time may be required for intact skin measurements.

Alternatively, Fig. 5b looks at TG while varying the receiver solution concentrations and keeping the MN treatment constant. The MN-treated skin data reveals unsteady-state diffusion of TG through full thickness pig skin in which TG concentration increases with time. It takes multiple hours for glucose concentrations in the system to begin to level off and reach a steady-state condition. It was observed that the slope increases with increasing mM receiver solution concentration. The calculated slopes provide the rate of increase in sample glucose concentration in which the lowest concentration (3 mM) has a rate of increase at 0.004 ± 0.006 μM min^{-1} and the highest concentration has one at 0.123 ± 0.066 μM min^{-1}. Similarly, when the TG diffusion rate versus time was plotted (not shown), we see an increase in the diffusion rate with time for each increase of the observed concentrations. The slopes calculated for this graph provide the diffusion's acceleration (μM/min^{-2}) which also increase with increasing mM receiver solution (not shown). Figure 6 shows that when the slopes in Fig. 5b (rate of increase of TG) were compared to corresponding mM concentrations of the receiver solution, a significant positive linear correlation ($r = 0.999$, $p < 1 \times 10^{-4}$, CI = 99.99%) was observed following the trend $[y = (0.003 \pm 7.150\text{E-}5)x + (-0.005 \pm 0.001)]$. The acceleration of the TG diffusion rate also showed a linear correlation to the mM glucose concentrations. Meaning instead of waiting for the system to reach steady state, the initial rates, or slopes,

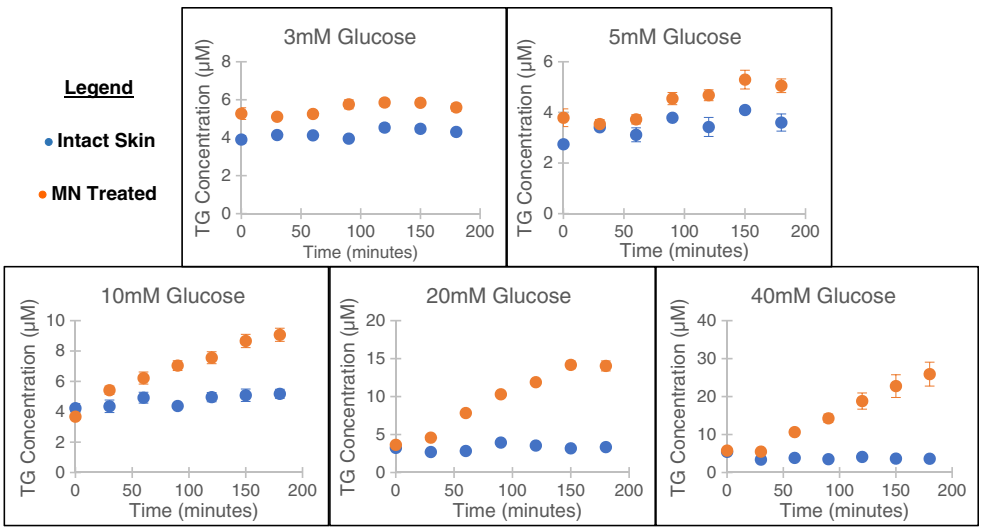

Fig. 4 Pig skin TG concentration for intact versus MN-treated skin for various clinically significant blood glucose concentrations

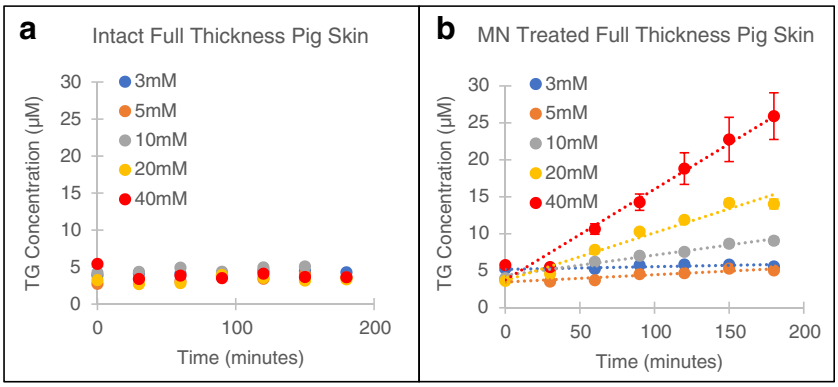

Fig. 5 TG concentrations (μM) of (**a**) intact and (**b**) MN-treated pig skin while varying receiving solution concentration (mM)

can be used to determine mM glucose concentrations from TG samples. This will be applicable for a point of care (POCT) GBP biosensor setup that continuously measures glucose similar to the biosensor setup described by Tiangco et al. [45].

Diffusion studies on healthy adults

In subsequent experiments, MNs were implemented into the transdermal sampling protocol for multiple healthy adult subjects. The change in the skin permeability with the implementation of MNs was determined by first measuring the skin diffusivity, or TEWL. To determine the ideal position for MN application on human subjects, the cyberDerm evaporimeter was used for measuring TEWL at two different skin sites, while varying number and length of MNs, as well as application time. Because of its high TEWL values, the fingertip previously showed success with noninvasive collection and measurement of TG in adults [22]; however, due to the thickness of the dermis at this site, no change in TEWL was observed with the application of MNs (Table 2). In addition, subjects experienced slight discomfort for MN lengths exceeding 250 μm. As an alternative, the forearm was used as a testing site. As expected, due to the presence of thinner dermis, the TEWL increased with increasing application time, length of MNs, and number of MNs (Table 2). Volunteers did experience slight discomfort for MN application times greater than 30 s and lengths exceeding 250 μm. For a 30-s application time, the 36 MN array showed an increase of TEWL from 3.73 to 21.06 g/m^2 h compared to the 9 MN array that increased only from 4.66 to 10.04 g/m^2 h. As a result, the 36 MN array, at a length of 250 μm, applied 30 s on the forearm was the most effective with no discomfort to subjects. To confirm these optimum MN parameters, TG samples were also measured on the forearm of a healthy adult while varying MN number and keeping the MN length and application time constant.

During the fasting phase, TG samples were collected from the forearm of a healthy adult after applying 250-μm MNs for

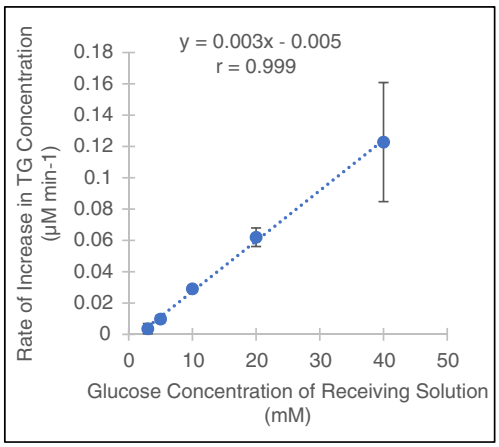

Fig. 6 Linear relationship observed when plotting receiving solution's mM concentrations to slope, or rate of increase in TG concentration following trend $y = (0.003 \pm 7.150\text{E-}5) + (-0.005 \pm 0.001)$ with a correlation coefficient of 0.999

Table 2 TEWL measurement on adult subjects varying MN application site, application time, and number

Fingertip		
(9 MN array, 250 μm)		
MN application time (s)	TEWL (g/m^2*h)	Standard deviation
0 (baseline)	44.66	5.35
5	44.55	0.45
30	37.01	1.83
Forearm		
(9 MN array, 250 μm)		
MN application time (s)	TEWL (g/m^2*h)	Standard deviation
0 (baseline)	4.66	0.29
5	8.82	0.57
30	10.04	0.23
60	13.16	1.07
120	18.47	0.87
(9 MN array, 500 μm)		
60	36.01	1.67
(36 MN array, 250 μm)		
0 (baseline)	3.73	0.11
30	21.06	0.07

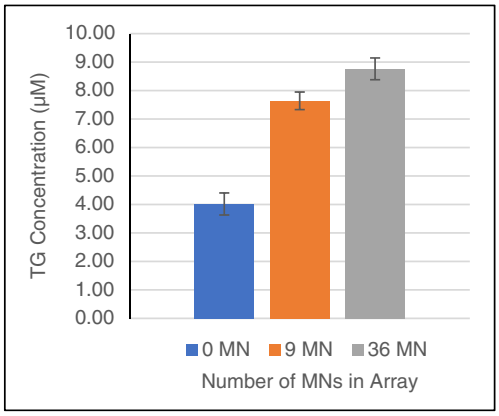

Fig. 7 TG concentrations of a healthy fasting adult subject collected while varying number of MNs in array

30 s. The tested MN array numbers included 0, 9, and 36 MNs. Figure 7 shows the measured TG concentrations associated with varying the number of MNs. The observed concentrations support the previous conclusion from the TEWL study that there is an increase in permeability of the skin with the use of MNs. The completely noninvasive sampling resulted in a TG concentration of 4.02 μM for intact human skin. When the MN array was applied, it was observed that there was an increase in the TG concentration as the number of MNs in the array increased. A maximum TG concentration of approximately 8.76 μM was observed revealing a more than double increase in TG concentration with the use of MNs. Although the measured TG for MN-treated skin is significantly higher than that of intact skin ($p < 1 \times 10^{-5}$), there was no significant difference detected between the TG concentrations observed when the 9 and 36 MN arrays were applied ($p > 0.05$). Ultimately, the 36 MN array was chosen for additional testing on human subjects due to there being no associated discomfort with its use. Both the diffusivity measurements and the corresponding TG measurements support that MN implementation increases human skin permeability allowing for detection of passively diffusing glucose.

Using the previously determined ideal MN parameters (250 μm, 36 MN array) and human skin testing site (forearm), TG was collected on another healthy adult subject during an OGTT. TG concentration and TEWL were monitored with and without using MNs on an adult subject during phases of fasting and high glucose levels. During this study, blood glucose was measured and compared to that of the collected and analyzed transdermal glucose. Transdermal samples were first noninvasively collected on uncompromised human skin (Fig. 8), followed by a minimally invasive collection using the vibrating MN pen with a 36 MN array insert (Fig. 9).

As previously mentioned, TEWL was measured to confirm penetration of MN through skin. For uncompromised adult human skin, the average measured TEWL was 0.81 ± 0.27 g m^{-2} h. Upon application with a 36 MN array, the TEWL increased almost 16 times to 13.53 ± 4.56 g m^{-2} h. The decrease in these TEWL values compared to those presented in Table 2 can be partially attributed to a different human subject being tested. In addition, a different evaporimeter device (Delfin VapoMeter) was used in lieu of accessibility issues to the originally used TEWL measuring device; however, the observed trend (increase in TEWL with MN application) for both devices remained similar.

The TG samples measured for both the intact and MN skin during the OGTT show a trend compared to corresponding blood glucose. Also, a statistically significant positive correlation exists when the TG is compared to blood glucose ($r \geq 0.95$, $p < 0.01$, CI $\geq 99.7\%$), where the TG of intact skin follows the trend $[y = (0.921 \pm 0.150)x + (-1.231 \pm 0.872)]$ and MN-treated skin follows the trend $[y = (1.530 \pm 0.217)x + (-0.496 \pm 1.247)]$. The collected data also shows that there is an almost doubling of TG concentration amounts collected and measured when the 36 MN array is used. This further supports what was previously observed for the TG concentrations of a fasting adult with and without the use of MNs.

For both the pig skin and human model, consistency of sampling was considered and monitored. Although applied MN pressure was not measured, diffusivity measurements were used to establish consistency in diffusion rate change across the skin barrier after MN application. We observed that after MN application, the actual TEWL values and sample concentration measured for pig and human skin showed larger deviation compared to intact skin. An F test comparing variation in TEWL for intact and MN-treated skin confirmed unequal

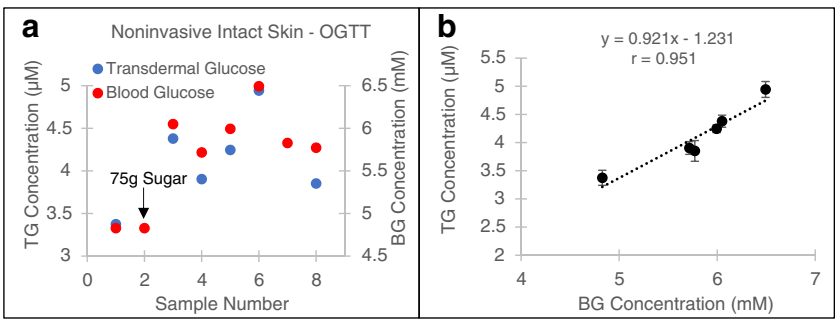

Fig. 8 (**a**) TG of intact skin being used to track blood glucose (BG) in a healthy adult subject. (**b**) Linear correlation between TG measured by biosensor and corresponding blood glucose following trend $y = (0.921 \pm 0.150)x + (-1.231 \pm 0.872)$ with a correlation coefficient of 0.951

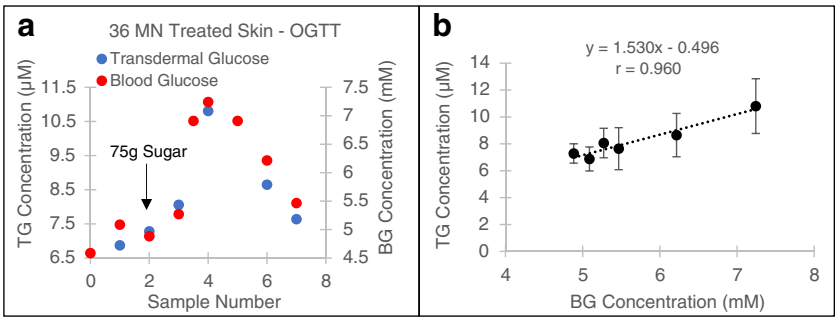

Fig. 9 (**a**) TG of MN-treated skin being used to track blood glucose (BG) in a healthy adult subject. (**b**) Linear correlation between TG and corresponding blood glucose following the trend $y = (1.530 \pm 0.217)x + (-0.496 \pm 1.247)$ with a correlation coefficient of 0.960

variance in which there was higher variation in the TEWL values for MN-treated skin. Although the adjustment ring of the vibrating MN pen was designed to minimize issues of varying pressure application by physicians or users [46, 47], the presented results suggest that some variance in applied pressure was present during the study. This can explain the larger error seen in sample concentrations collected from MN skin. The pressure variability can be a result of the device's vibrating motion causing the adjustment ring to not sit consistently on the skin surface. This suggests that a one-press MN application system can possibly be used in the future to reduce this variability. Future work can look at implementing a lancing device that allows for one-time insertion of needle instead of vibrating. The presence of the adjustment ring can help to standardize the starting position of the needles prior to insertion. The removal of the vibrating motion can eliminate the issue for the adjustable ring to not consistently rest on skin surface.

Conclusion

In this work, we present a minimally invasive sampling protocol that allows for tracking of blood glucose through passively diffused transdermal glucose levels. The implementation of MNs allows for an increased permeability in the skin models studied. There is an increase in the diffusion of glucose across the skin because of the removal of the permeability limitations caused by the stratum corneum. As a result, higher concentrations of transdermal glucose can be collected and measured by the highly sensitive GBP biosensor. The micromolar sensitivity of the biosensor ($K_d = 0.67$) reduced the ISF volume required for glucose analysis and minimized the time required for MN application (30 s), which was shorter than previously reported where the MNs were placed in the skin anywhere from a few minutes up to an hour [32]. In addition, because of the increased skin permeability and TG diffusion, the transdermal sampling protocol collection time can be decreased. MNs used for ISF glucose monitoring are left in the skin for prolonged times and can result in skin irritation. The shortened application time helps in reducing this irritation. Also, the use of PBS buffer in the unique protocol reported here for TG collection allowed for passive diffusion of ISF glucose, eliminating the need for vacuum suction or other ISF extraction techniques. During the study, the vibrating MN application did cause some variability in the TEWL values measured, as seen by the large standard deviation. Future work can involve using a one-press application system to address this variability. In addition, studies on adult subjects looking at additional sites for MN application may help in optimizing this minimally invasive technique for use in the pediatric age group. The his-tagged micromolar biosensor presented in this work can be immobilized and used with a portable sensing fluorometer device at the point of care, making this minimally invasive technology more ideal for use in the PICU. The increased TG diffusion associated with implementing MNs can help in shortening the time of the sampling and measuring protocol to be used by caregivers in the hospital.

Acknowledgements The authors acknowledge the Eunice Kennedy Shriver National Institute of Child Health and Human Development for grant R41HD088223 and the UMB-UMBC Research and Innovation Partnership Grant Program for project funding, as well as, the UMBC Meyerhoff Graduate Program and LSAMP Bridges to the Doctorate Program for S. Brown's funding. The authors would like to thank Dr. Russel Potts for invaluable input and Eric Ankers for assistance with experimental work.

Compliance with ethical standards

The authors declare no conflict of interest. Yucatan minipig skin was purchased from Sinclair BioResources who comply with multiple agencies and are a USDA licensed breeder (43-A-5793). The company is in full compliance with the Animal Welfare Act and has maintained accreditation by the Association for Assessment and Accreditation of Laboratory Animal Care International (AAALAC International) since 1995.

The studies on human subjects were conducted in accordance with the Declaration of Helsinki, and the protocol was approved by the Office of Research Protections and Compliance of UMBC (Protocol Y17LT05060) on November 9, 2016.

References

1. Wolfsdorf J, Craig ME, Daneman D, Dunger D, Edge J, Lee W, et al. Diabetic ketoacidosis in children and adolescents with diabetes. Pediatr Diabetes. 2009;10:118–33. https://doi.org/10.1111/j.1399-5448.2009.00569.x.

2. Piper HG, Alexander JL, Shukla A, Pigula F, Costello JM, Laussen PC, et al. Real-time continuous glucose monitoring in pediatric patients during and after cardiac surgery. Pediatrics. 2006;118(3): 1176–84. http://www.ncbi.nlm.nih.gov/pubmed/16951013
3. Allen HF, Rake A, Roy M, Brenner D, McKiernan CA. Prospective detection of hyperglycemia in critically ill children using continuous glucose monitoring*. Pediatr Crit Care Med. 2008;9(2):153–8. https://insights.ovid.com/crossref?an=00130478-200803000-00003
4. Joseph JI, Hipszer B, Mraovic B, Chervoneva I, Joseph M, Grunwald Z. Clinical need for continuous glucose monitoring in the hospital. J Diabetes Sci Technol. 2009;33(66): 1309–18. https://doi.org/10.1177/193229680900300611.
5. Bridges BC, Preissig CM, Maher KO, Rigby MR. Continuous glucose monitors prove highly accurate in critically ill children https://ccforum.biomedcentral.com/track/pdf/10.1186/cc9280
6. Barrio Castellanos R, Harris DL, Battin MR, Weston PJ, Harding JE. Continuous glucose monitoring in newborn babies at risk of hypoglycemia. Av en Diabetol. 2010;26(3):209–10. https://doi.org/10.1016/j.jpeds.2010.02.003.
7. Signal M, Pretty CG, Chase JG, Le Compte A, Shaw GM. Continuous glucose monitors and the burden of tight glycemic control in critical care: can they cure the time cost? J Diabetes Sci Technol. 2010;4(3):625–35. Available from: http://www.pubmedcentral.nih.gov/articlerender.fcgi?artid=2901040&tool=pmcentrez&rendertype=abstract
8. Pretty CG, Chase JG, Le Compte A, Shaw GM, Signal M. Hypoglycemia detection in critical care using continuous glucose monitors: an in silico proof of concept analysis. J Diabetes Sci Technol. 2010;4(1):15–24. Available from: http://www.pubmedcentral.nih.gov/articlerender.fcgi?artid=2825620&tool=pmcentrez&rendertype=abstract
9. Beardsall K, Ogilvy-Stuart AL, Ahluwalia J, Thompson M, Dunger DB. The continuous glucose monitoring sensor in neonatal intensive care. Arch Dis Child Fetal Neonatal Ed. 2005;90(4):F307–10. Available from: http://fn.bmj.com/content/90/4/F307.long
10. Wintergerst KA, Foster MB, Sullivan JE, Woods CR, Affiliations A. Association of hyperglycemia, glucocorticoids, and insulin use with morbidity and mortality in the pediatric intensive care unit. J Diabetes Sci Technol. 2012;6(1) https://doi.org/10.1177/193229681200600102.
11. Wintergerst KA, Buckingham B, Gandrud L, Wong BJ, Kache S, Wilson DM. Association of hypoglycemia, hyperglycemia, and glucose variability with morbidity and death in the pediatric intensive care unit. Pediatrics. 2006;118(1):173–9. Available from: http://www.ncbi.nlm.nih.gov/pubmed/16818563
12. Ge X, Rao G, Tolosa L. On the possibility of real-time monitoring of glucose in cell culture by microdialysis using a fluorescent glucose binding protein sensor. Biotechnol Prog. 2008;24(3):691–7.
13. Ge X, Tolosa L, Rao G. Dual-labeled glucose binding protein for ratiometric measurements of glucose. Anal Chem. 2004;76(5): 1403–10.
14. Ge X, Rao G, Kostov Y, Kanjananimmanont S, Viscardi RM, Woo H, et al. Detection of trace glucose on the surface of a semipermeable membrane using a fluorescently labeled glucose-binding protein: a promising approach to noninvasive glucose monitoring. J Diabetes Sci Technol. 2013;7(1): 4–12. http://www.pubmedcentral.nih.gov/articlerender.fcgi?artid=3692211&tool=pmcentrez&rendertype=abstract
15. Ge X, Lam H, Modi SJ, LaCourse WR, Rao G, Tolosa L. Comparing the performance of the optical glucose assay based on glucose binding protein with high-performance anion-exchange chromatography with pulsed electrochemical detection: efforts to design a low-cost point-of-care glucose sensor. J Diabetes Sci Technol. 2007;1(6):864–72.
16. Fonin AV, Stepanenko OV, Povarova OI, Volova CA, Philippova EM, Bublikov GS, et al. Spectral characteristics of the mutant form GGBP/H152C of D-glucose/D-galactose-binding protein labeled with fluorescent dye BADAN: influence of external factors. PeerJ. 2014;2:e275. Available from: https://peerj.com/articles/275
17. Khan F, Saxl TE, Pickup JC. Fluorescence intensity- and lifetime-based glucose sensing using an engineered high-Kd mutant of glucose/galactose-binding protein. Anal Biochem. 2010;399(1): 39–43. https://www.sciencedirect.com/science/article/pii/S0003269709008112
18. Joel S, Turner KB, Daunert S. Glucose recognition proteins for glucose sensing at physiological concentrations and temperatures. ACS Chem Biol. 2014;9(7):1595–602. https://doi.org/10.1021/cb500132g.
19. Quiocho FA. Atomic structures of periplasmic binding proteins and the high-affinity active transport systems in bacteria. Philos Trans R Soc Lond Ser B Biol Sci. 1990;326(1236):341–52. http://www.ncbi.nlm.nih.gov/pubmed/1970641
20. Ge X, Tolosa L, Simpson J, Rao G. Genetically engineered binding proteins as biosensors for fermentation and cell culture. Biotechnol Bioeng. 2003;84(6):723–31.
21. Salins LL, Ware RA, Ensor CM, Daunert S. A novel reagentless sensing system for measuring glucose based on the galactose/glucose-binding protein. Anal Biochem. 2001;294(1):19–26.
22. Kanjananimmanont S, Ge X, Mupparapu K, Rao G, Potts R, Tolosa L. Passive diffusion of transdermal glucose: noninvasive glucose sensing using a fluorescent glucose binding protein. J Diabetes Sci Technol. 2014;8(2):291–8. http://www.ncbi.nlm.nih.gov/pubmed/24876581
23. Tiangco C, Andar A, Quarterman J, Ge X, Sevilla Iii F, Rao G, et al. Measuring transdermal glucose levels in neonates by passive diffusion: an in vitro porcine skin model. Anal Bioanal Chem. 2017;409: 3475–82. https://link.springer.com/content/pdf/10.1007%2Fs00216-017-0289-7.pdf
24. Khanna P, Strom JA, Malone JI, Bhansali S. Microneedle-based automated therapy for diabetes mellitus. J Diabetes Sci Technol. 2008;2(6):1122–9. Available from: http://dst.sagepub.com/content/2/6/1122.abstract
25. Teo AL, Shearwood C, Ng KC, Lu J, Moochhala S. Transdermal microneedles for drug delivery applications. Mater Sci Eng B. 2006;132(1–2):151–4.
26. Yadav JD, Vaidya KA, Kulkarni PR, Raut RA. Microneedles: promising technique for transdermal drug delivery. Int J Pharm Bio Sci. 2011;2:684–708.
27. Henry S, McAllister DV, Allen MG, Prausnitz MR. Microfabricated microneedles: a novel approach to transdermal drug delivery. J Pharm Sci. 1998;87(8):922–5. http://linkinghub.elsevier.com/retrieve/pii/S0022354915506242
28. Wang PM, Cornwell M, Prausnitz MR. Minimally invasive extraction of dermal interstitial fluid for glucose monitoring using microneedles. Diabetes Technol Ther. 2005;7(1):131–41. https://doi.org/10.1089/dia.2005.7.131.
29. Sakaguchi K, Hirota Y, Hashimoto N, Ogawa W, Sato T, Okada S, et al. A minimally invasive system for glucose area under the curve measurement using interstitial fluid extraction technology: evaluation of the accuracy and usefulness with oral glucose tolerance tests in subjects with and without diabetes. Diabetes Technol Ther. 2012;14(6):485–91. https://doi.org/10.1089/dia.2011.0255.
30. Donnelly RF, Mooney K, Caffarel-Salvador E, Torrisi BM, Eltayib E, McElnay JC. Microneedle-mediated minimally invasive patient monitoring. Ther Drug Monit. 2013; http://content.wkhealth.com/linkback/openurl?sid=WKPTLP:landingpage&an=00007691-900000000-99442

31. Romanyuk AV, Zvezdin VN, Samant P, Grenader MI, Zemlyanova M, Prausnitz MR. Collection of analytes from microneedle patches. Anal Chem. 2014;86(21):10520–3. https://doi.org/10.1021/ac503823p.
32. Caffarel-Salvador E, Brady AJ, Eltayib E, Meng T, Alonso-Vicente A, Gonzalez-Vazquez P, et al. Hydrogel-forming microneedle arrays allow detection of drugs and glucose in vivo: potential for use in diagnosis and therapeutic drug monitoring. Chan C, editor. PLoS One. 2015;10(12):e0145644. Available from: http://journals.plos.org/plosone/article/file?id=10.1371/journal.pone.0145644&type=printable
33. Chang H, Zheng M, Yu X, Than A, Seeni RZ, Kang R, et al. A swellable microneedle patch to rapidly extract skin interstitial fluid for timely metabolic analysis. Adv Mater. 2017;29(37):1702243. https://doi.org/10.1002/adma.201702243.
34. Kiang T, Ranamukhaarachchi S, Ensom M. Revolutionizing therapeutic drug monitoring with the use of interstitial fluid and microneedles technology. Pharmaceutics. 2017;9(4):43. http://www.ncbi.nlm.nih.gov/pubmed/29019915
35. Zimmermann S, Fienbork D, Stoeber B, Flounders AW, Liepmann D. A microneedle-based glucose monitor: fabricated on a wafer-level using in-device enzyme immobilization. In: TRANSDUCERS'03 12th International Conference on Solid-State Sensors, Actuators and Microsystems Digest of Technical Papers (Cat No03TH8664). IEEE;. p. 99–102. http://ieeexplore.ieee.org/document/1215262/
36. Zimmermann S, Fienbork D, Flounders AW, Liepmann D. In-device enzyme immobilization: wafer-level fabrication of an integrated glucose sensor. Sensors Actuators B. 2004;99:163–73. Available from: https://ac.els-cdn.com/S0925400503005525/1-s2.0-S0925400503005525-main.pdf?_tid=020881da-3da9-4b06-84bf-c64ada008838&acdnat=1533673088_35e97cd3db5f6bd17c320720a55d18b0
37. Mukerjee EV, Collins SD, Isseroff RR, Smith RL. Microneedle array for transdermal biological fluid extraction and in situ analysis. Sensors Actuators A. 2004;114:267–75. Available from: https://ac.els-cdn.com/S0924424703006381/1-s2.0-S0924424703006381-main.pdf?_tid=516bf37c-6980-4149-88a5-63fb8c136f85&acdnat=1533668749_77d67ae1d55cee1ddb39130ed33ed624
38. Strambini LM, Longo A, Scarano S, Prescimone T, Palchetti I, Minunni M, et al. Self-powered microneedle-based biosensors for pain-free high-accuracy measurement of glycaemia in interstitial fluid. 2014; Available from: https://doi.org/10.1016/j.bios.2014.11.010
39. Sharma S, Huang Z, Rogers M, Boutelle M, Cass AEG. Evaluation of a minimally invasive glucose biosensor for continuous tissue monitoring. Anal Bioanal Chem. 2016;408(29):8427–35. https://doi.org/10.1007/s00216-016-9961-6.
40. Jina A, Tierney MJ, Tamada JA, McGill S, Desai S, Chua B, et al. Design, development, and evaluation of a novel microneedle array-based continuous glucose monitor. J Diabetes Sci Technol. 2014;8(3):483–7. Available from: http://www.pubmedcentral.nih.gov/articlerender.fcgi?artid=4455438&tool=pmcentrez&rendertype=abstract
41. Chua B, Desai SP, Tierney MJ, Tamada JA, Jina AN. Effect of microneedles shape on skin penetration and minimally invasive continuous glucose monitoring in vivo. Sensors Actuators A Phys. 2013;203:373–81. https://doi.org/10.1016/j.sna.2013.09.026.
42. Lam H, Kostov Y, Rao G, Tolosa L. Low-cost optical lifetime assisted ratiometric glutamine sensor based on glutamine binding protein. Anal Biochem. 2008;383(1):61–7.
43. Gupta VK, Zatz JL, Rerek M. Percutaneous absorption of sunscreens through micro-Yucatan pig skin in vitro. Pharm Res. 1999;16(10):1602–7. https://doi.org/10.1023/A:1018916907263.
44. Milewski M. Microneedle-assisted transdermal delivery of naltrexone species: in vitro permeation and in vivo pharmacokinetics studies. Vol. 160. University of Kentucky Doctoral Dissertations; 2011. Available from: https://uknowledge.uky.edu/gradschool_diss/160
45. Tiangco C, Fon D, Sardesai N, Kostov Y, Sevilla F, Rao G, et al. A fiber optic biosensor for umolar levels of glucose less figures. Sensors Actuators. 2015;
46. Bhatnagar S, Dave K, Venuganti VVK. Microneedles in the clinic. J Control Release. 2017;260:164–82. Available from: https://www.sciencedirect.com/science/article/pii/S016836591730603X
47. McCrudden MTC, McAlister E, Courtenay AJ, González-Vázquez P, Raj Singh TR, Donnelly RF. Microneedle applications in improving skin appearance. Exp Dermatol. 2015;24(8):561–6. https://doi.org/10.1111/exd.12723.